Spectral Hole Burning and Fluorescence Line Narrowing in Subunits of the Light-Harvesting Complex LH1 of Purple Bacteria

T. M. H. Creemers,[†] C. A. De Caro,[†,‡] R. W. Visschers,[§] R. van Grondelle,[||] and S. Völker*,[†,||]

Center for the Study of Excited States of Molecules, Huygens and Gorlaeus Laboratories, University of Leiden, 2300 RA Leiden, The Netherlands, Department of Biomolecular Structure and Dynamics, Faculty of Biology, Free University, 1081 HV Amsterdam, The Netherlands, and Department of Biophysics, Faculty of Exact Sciences, Free University, 1081 HV Amsterdam, The Netherlands

Spectroscopic properties of the B820 and B777 subunits of the core light-harvesting complex LH1 of purple bacteria *Rhodospirillum rubrum G9* were studied by hole burning (HB) and fluorescence line narrowing (FLN) between 1.2 and 4.2 K. We have found that an equilibrium exists between the three forms B820, B777, and the native LH1-complex in the presence of the detergent *n*-octyl-β-D-glucopiranoside (OG). The shift of this equilibrium was followed as a function of OG concentration by means of absorption and fluorescence spectra. Low-frequency modes at 19 cm^{-1} for B820 and at 25 cm^{-1} for B777 were identified by FLN. From the spectral position of these modes as a function of excitation wavelength λ_{exc} and from the homogeneous line width Γ'_{hom} as a function of λ_{exc}, we conclude that "downhill" energy transfer does not take place either among B820 or among B777 subunits. The temperature dependence of Γ'_{hom}, however, indicates that optical dephasing and/or spectral diffusion does occur in these subunits. The positions of side holes and antiholes, furthermore, suggest that the hole-burning mechanisms in B820 and B777 are similar, although their HB efficiencies differ by a factor of 10.

1. Introduction

Light-harvesting (LH) complexes in purple bacteria are responsible for the efficient collection of sun light and the transfer of excitation energy to the reaction center (RC) in photosynthesis. The primary charge separation occurs in the RC and leads to the subsequent conversion of excitation energy into a chemically useful form. Most purple bacteria contain two types of LH complexes: the LH1 core complex surrounding each RC and peripheral LH2 complexes which absorb slightly further to the blue and transfer the excitation energy to LH1.[1] Both the LH1 and LH2 complexes have ringlike structures[2,3] containing a basic repeating subunit. This subunit consists of a dimer of bacteriochlorophyll-*a* (BChl-*a*) molecules bound to two helical polypeptides (α and β), each comprising ∼50 amino acids[4] with a protein mass of approximately 6 kDa. The circular arrangement of the reconstituted LH1 in *Rhodospirillum rubrum G9* is built up from 16 subunits. It has an outer diameter of 116 Å and an inner diameter of 68 Å, probably enclosing the RC.[2] The LH1 complex (B873) can be reversibly dissociated into its constituent subunits by detergent titration.[5,6] The detergent, *n*-octyl-β-D-glucopyranoside (OG), forms micelles which enclose either the dimeric subunit, called B820 (if ∼1.2% OG is used) or the B777 monomer subunit (when ∼5% OG is used). Reassociation of the subunits yields an aggregate with a spectrum nearly identical to that of LH1.[5,7]

Although the absorption spectrum and the fluorescence lifetime of B777 are similar to those of BChl-*a* in solution,[8,9]

its Raman spectrum is not.[10] This has led to a controversy in the literature, namely whether the BChl-*a* molecule in B777 is noncovalently bound to the protein or is "free". Recently, we have proven by means of time-resolved hole burning that under our experimental conditions (see section 2.1) it is indeed bound to the protein.[11]

The three complexes B873, B820, and B777 are supposed to be in equilibrium at room temperature in the presence of the OG detergent:[10]

$$\text{B873} \leftrightarrow n \text{ B820} \leftrightarrow 2n \text{ B777} \qquad (1)$$
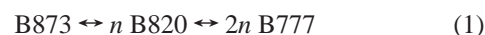
where $n \sim 16$ is the oligomer size.[2,12] By increasing the OG concentration or the temperature, the equilibrium is driven toward the monomeric form. This process is reversible. We will show that at low temperature the presence of very small amounts of any of the three complexes can be detected by using sensitive optical techniques, like fluorescence spectroscopy. Furthermore, we have identified low-frequency modes in B820 and B777 by means of fluorescence line narrowing (FLN). The emission wavelengths of these modes as a function of excitation wavelength yield information on energy transfer processes within the Q_y absorption band. We have also found that hole burning is feasible in both B820 and B777 subunits, which proves that their absorption bands are inhomogeneously broadened at low temperature. By comparing the positions of side holes and antiholes burned in B820 and B777, we have inferred the hole-burning mechanism in these complexes. Finally, we have obtained the "effective" homogeneous line width Γ'_{hom} from the burning-fluence density dependence of the hole width. Conclusions are drawn about optical dephasing and energy transfer processes in these subunits of LH1 from the variation of Γ'_{hom} with temperature and excitation wavelength.

* To whom correspondence should be addressed.
† University of Leiden.
‡ Current adress: Mettler-Toledo GmbH Analytical, Sonnenbergstrasse 74, CH-8603 Schwerzenbach, Switzerland.
§ Department of Biomolecular Structure and Dynamics, Faculty of Biology.
|| Department of Biophysics, Faculty of Exact Sciences.

Spectral Hole Burning and Fluorescence Line Narrowing

J. Phys. Chem. B, Vol. 103, No. 44, 1999 **9771**

2. Experimental Section

2.1 Sample Preparation. Cells of *Rs. rubrum G9*, a carotenoidless mutant, were grown anaerobically for 3−5 days under continuous illumination. They were harvested by centrifugation and broken by three passes through a French press in the presence of DNA-ase (10 μg/ml), then layered onto sucrose gradients (45−15%) and spun for 6 h at 170.000 G. The blue chromatophore fraction was collected and stored in liquid nitrogen.[13] For the preparation of B820 subunits, the chromatophores were thawed and diluted to an optical density $OD_{880} \approx$ 5 cm^{-1}. The detergent *n*-octyl-β-D-glucopiranoside (OG, from Sigma) was added (1−1.2% OG) until conversion to the B820 form was observed. The sample was subsequently centrifuged at 40.000 G for 1 h to remove insoluble material. The B820 complexes were concentrated to an $OD_{820} \sim 20-40$ cm^{-1} using concentration tubes (Centriprep-10, Amicon Inc.). Subsequently, the complexes were applied to a FPLC gel filtration column (Superose-12, Pharmacia Inc.) equilibrated with 20 mM Tris buffer pH 8.0, containing 100 mM NaCl and 1% OG. This step separates reaction centers from the B820 subunits on the basis of molecular weight.[14] "Pure" B820 fractions with OD_{820}/OD_{777} > 4 were collected.

To obtain transparent samples for low-temperature measurements, the B820 fractions were diluted into 20 mM Tris buffer, pH 8.0, containing 100 mM NaCl and 65−75% (v/v) glycerol. Mixtures of B777, B820, and B873 were obtained by adding various amounts of OG (between 0.6% and 5%) to the samples. "Pure" B873 aggregates were made by overnight dialysis of B820 fractions against buffer without OG. The final optical density (OD) of the samples at the maximum of the spectra was OD $\sim 0.1-1.0$ cm^{-1}, corresponding to concentrations $c\sim$ 0.1−0.3 μM for B873, $\sim$2−6 μM for B820, and $\sim$5−10 μM for B777. To estimate the concentrations, we used the extinction coefficients reported in ref 8 and assumed that B820 contains two BChl, whereas B873 contains 32 BChl. All samples were prepared in the dark and stored in liquid nitrogen.

The samples were placed in 3-mm thick cuvettes for experiments at liquid helium temperatures. To avoid cracks, they were kept in an empty ^{4}He bath cryostat of which the outer mantle was filled with liquid nitrogen. Subsequently, the cryostat was filled with liquid helium. The temperature of the sample, which was varied between 1.2 and 4.2 K by pumping on the ^{4}He vapor pressure, was measured with an accuracy better than 0.01 K using a calibrated carbon resistor in contact with the sample.

2.2 Absorption, Fluorescence, and Hole Burning Spectroscopy. Absorption spectra at 1.6 K (see Figure 1) were taken by irradiating the sample with a halogen lamp. The transmission signal of the sample was passed through a 0.85 m double-monochromator (SPEX 1402, resolution $\sim$10 cm^{-1}) and detected with a liquid nitrogen cooled photomultiplier with an S_1 cathode (EMI 9684). Absorption spectra were taken before and after each experiment to check whether or not the sample had degraded.

The broadband fluorescence and the fluorescence line narrowing (FLN) spectra (see Figures 2 and 3) were taken by irradiating the sample with a cw Ti:sapphire laser (Coherent 899-21, *without* intracavity assembly, bandwidth $\sim$6 GHz $\approx$ 0.2 cm^{-1}, intensity stabilized to $\leq$ 0.5%). While the frequency of the laser was fixed, the 0.85 m double monochromator was scanned. For broadband emission spectra, the resolution was $\sim$10 cm^{-1}; for FLN spectra it was $\sim$2 cm^{-1}. The intensity of the laser was sufficiently low to avoid burning while scanning the monochromator.
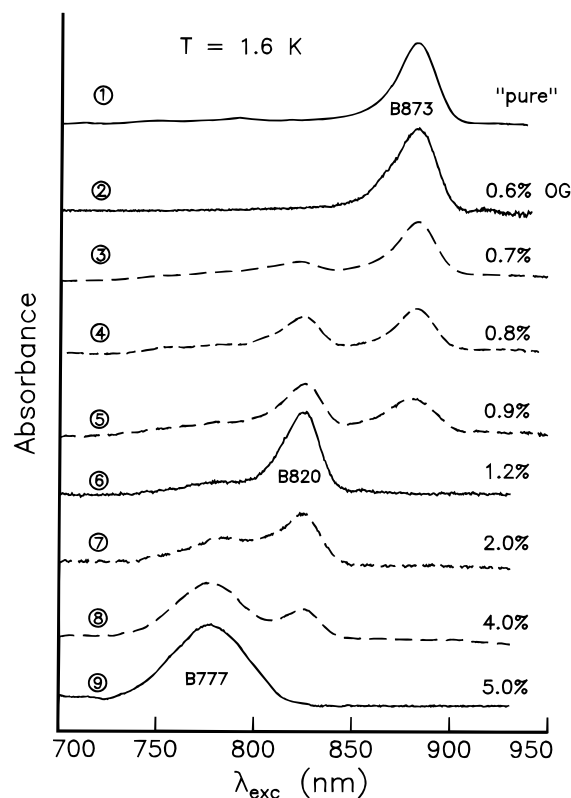

Figure 1. Absorption spectra of the B873 aggregate (LH1) and the subunits B820 (dimer) and B777 (monomer) of the LH1 complex of *Rs. rubrum G9* at 1.6 K, for various detergent (OG) concentrations.
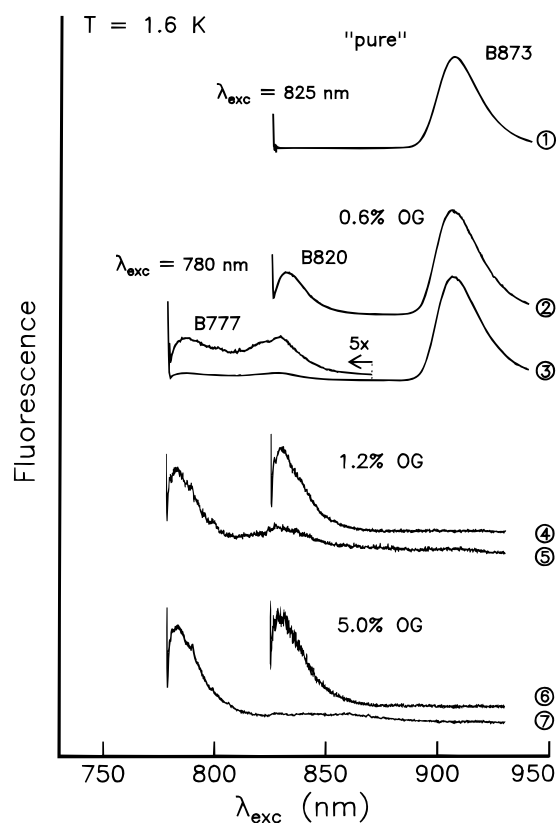

Figure 2. Fluorescence spectra for various concentrations of OG detergent at 1.6 K; excitation at $\sim$825 nm (maximum of B820) and $\sim$780 nm (maximum of B777).

Hole burning (HB) experiments were performed using the same cw Ti:sapphire laser, but in its single-frequency version

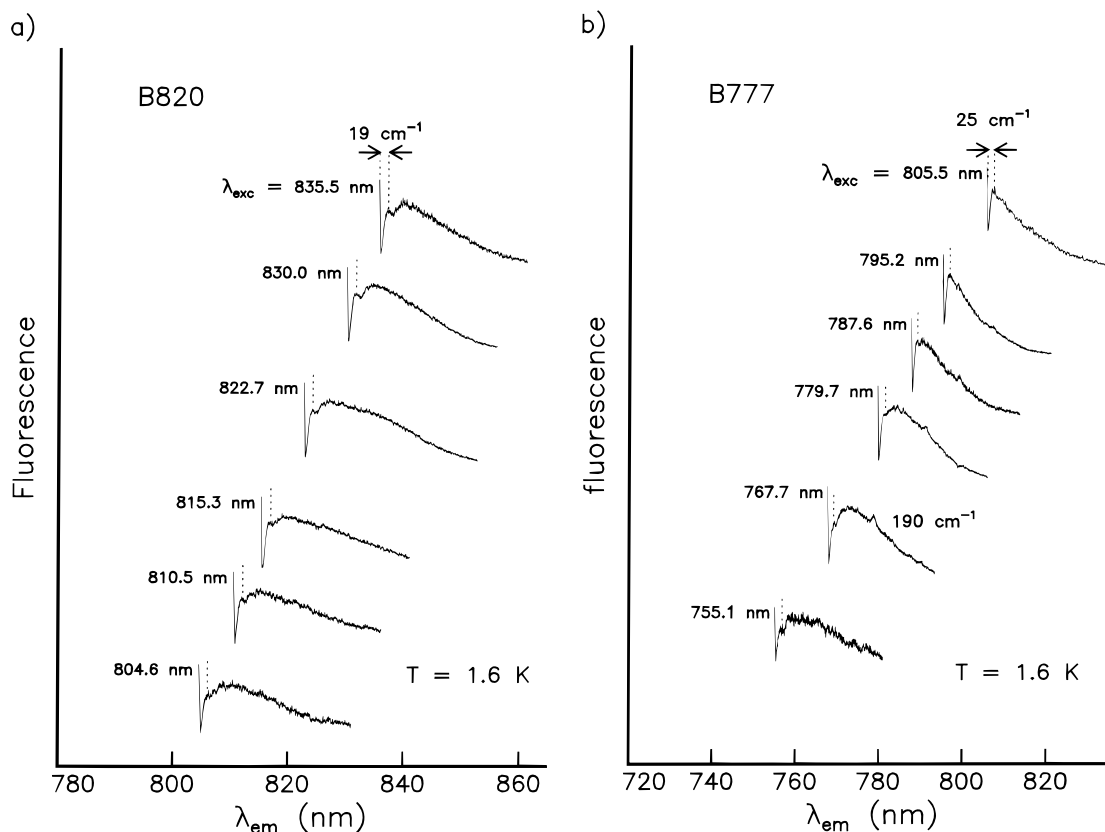**Figure 3.** Fluorescence line narrowing (FLN) spectra of (a) B820 and (b) B777 at 1.6 K for various excitation wavelengths λ_{exc}. A low-frequency mode is observed at 19 cm^{-1} in B820 and at 25 cm^{-1} in B777. In addition, a 190 cm^{-1} mode appears in B777 (marked only for λ_{exc} = 767.7 nm).
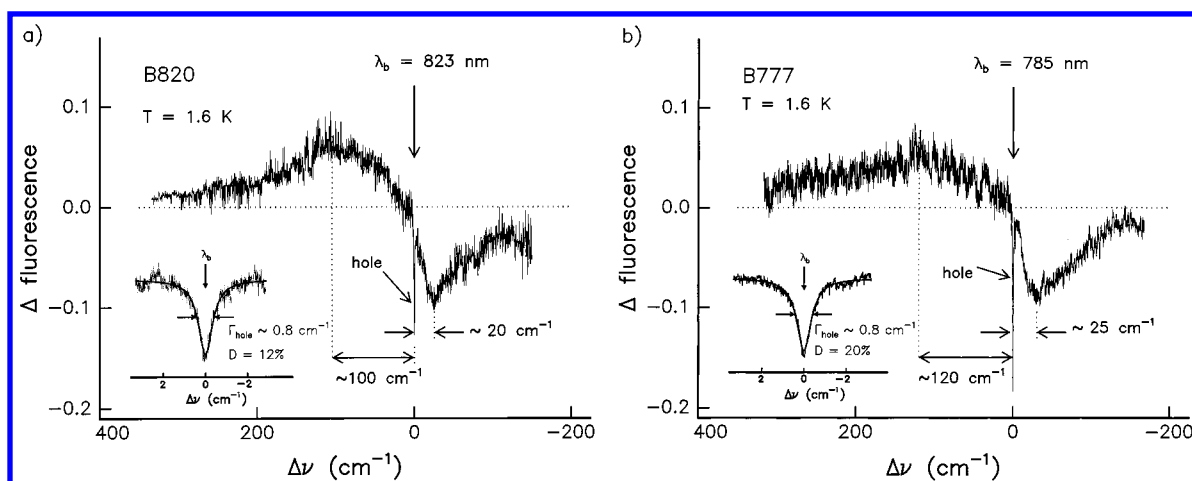

Figure 4. Change of the intensity of the fluorescence excitation spectra after burning a deep hole into B820 (a) and B777 (b) at 1.6 K. The insets show an amplification of the zero-phonon holes. They do not reflect the homogeneous line width due to burning fluence broadening. The phonon side hole is shifted by ~20 cm^{-1} to the red of the burned hole in B820 and by ~25 cm^{-1} in B777. The antihole is on the blue side of the burned hole at ~100 cm^{-1} for B820 and at 120 cm^{-1} for B777.

(Coherent 899-21 or -29, *with* intracavity assembly, frequency jitter ~0.5 MHz). Scans longer than 1 cm^{-1} (30 GHz) and up to 400 cm^{-1} (12 THz) were made using the autoscan option with a resolution in spectral position varying between ~25 and ~250 MHz, depending on the length of the scan. In this way, power-broadened holes, side holes, and antiholes were recorded (see Figure 4a,b). Short scans up to 30 GHz were performed without the autoscan option (jitter ~0.5 MHz) to obtain the "effective" homogeneous line width Γ'_{hom} (of ~0.5 to a few GHz at low temperature, see Figures 5 and 6). In these short scans, burning power densities between 3 and 600 μW/cm^2 with a burning time of t_b = 130 s were used. The holes were probed in fluorescence excitation with the same laser, but with its power

attenuated by a factor of about 100. The delay time between burning and probing the holes was fixed at t_d = 130 s. The fluorescence signals of the holes were detected with a photomultiplier (EMI 9684 or EMI 9658 R) and, subsequently, amplified. The signals were averaged point-by-point about 1000 times with a PC, with a total of 250 points.

The pulse sequence for hole burning experiments was as follows: first, a baseline over the spectral region of interest was obtained by scanning the frequency of the laser. Then, the frequency was fixed and a hole was burned at higher intensity during a time t_b. In the final step, after a delay time t_d, the profile of the hole was probed by scanning the frequency of the laser again at low intensity. The shape of the hole was obtained by
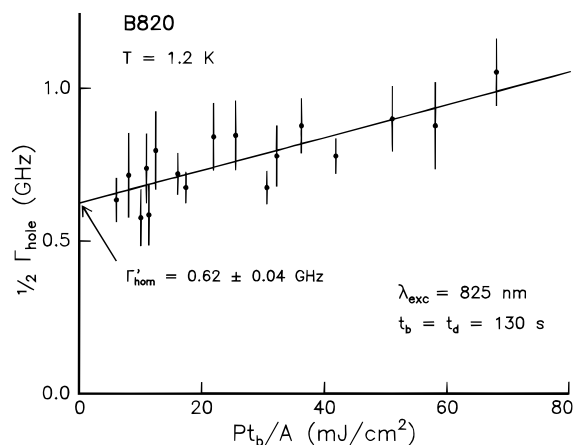
Figure 5. Half the hole width $1/2\ \Gamma_{hole}$ as a function of burning fluence density Pt_b/A (with P the burning power, t_b the burning time and A the area of the laser spot on the sample) for B820 at 1.2 K, $t_b = t_d = 130$ s (where t_d is the delay time between burning and probing the hole), and $\lambda_{exc} = 825$ nm. The "effective" homogeneous line width Γ'_{hom} is obtained by extrapolation of $1/2\ \Gamma_{hole}$ to $Pt_b/A \rightarrow 0$.
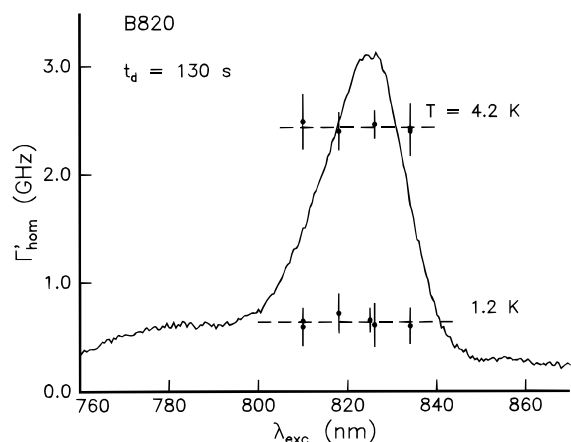

Figure 6. Dependence of Γ'_{hom} on excitation wavelength λ_{exc} for B820 at 1.2 and 4.2 K. At a given temperature, Γ'_{hom} is constant as a function of λ_{exc}, proving that "downhill" energy transfer does not take place within the Q_y absorption band. Since the value of Γ'_{hom} is larger at 4.2 K than at 1.2 K, there is optical dephasing and/or spectral diffusion.[11,16−18]

subtracting the signals before and after burning.[15−18] The holes were well fit by Lorentzian line shapes.

2.3 Determination of the "Effective" Homogeneous Line Width Γ'_{hom}. To obtain the "effective" homogeneous line width Γ'_{hom} (t_d), we have measured the hole width Γ_{hole} (t_b,t_d) as a function of burning fluence density Pt_b/A (where P is the burning power of the laser, t_b the burning time, t_d the delay time between burning and probing the hole, and A the area of the laser spot on the sample) and extrapolated the data to $Pt_b/A \rightarrow 0$ to eliminate the effect of power broadening (see section 3.4). Since the hole shapes are Lorentzian, the extrapolated value $\Gamma_{hole,0}$ (t_b,t_d) is given by[16−18]

$$\Gamma_{hole,0}\ (t_b,t_d) = \Gamma'_{hom}\ (t_b) + \Gamma'_{hom}\ (t_d) + 2\,\Gamma_{laser} \qquad (2)$$

where $\Gamma_{laser} \approx 0.5$ MHz corresponds to the jitter of the Ti:sapphire laser. Under the condition that $t_b = t_d$ as used here, Γ'_{hom} (t_d) becomes

$$\Gamma'_{hom}\ (t_d) = 1/2\ \Gamma_{hole,0}\ (t_b, t_d = t_b) - \Gamma_{laser} \qquad (3)$$

3. Results and Discussion

3.1 Equilibrium between B873, B820, and B777: Dependence on Detergent Concentration. Figure 1 shows absorption spectra between 700 and 950 nm of samples containing different mixtures of B873, B820, and B777 at 1.6 K. They were prepared at various concentrations of the OG detergent, with optical densities between OD∼ 0.3 and 1 cm^{-1}. At low concentration ($\leq$ 0.6% OG), a single absorption band is observed which corresponds to the B873 aggregate (compare spectra 1 and 2). Its maximum lies at ∼882 nm and its width is ∼340 cm^{-1}. This spectrum is identical to that found for intact carotenoidless LH1 complexes.[5,6] For detergent concentrations between 0.6 and ∼1.0% (spectra 3−5), a second absorption band appears with a maximum at 825 nm and a width of ∼320 cm^{-1}, which is the result of the formation of B820 dimer subunits. The equilibrium between B820 and B873 strongly depends on OG concentration: while the intensity of the B820 absorption band increases with OG concentration, that of B873 decreases. At 1.2% OG (spectrum 6), there is no detectable absorption of B873 anymore and the equilibrium is completely shifted toward B820. The absorption band of B820 is asymmetric. The red wing is somewhat steeper than the blue wing because on the blue side vibrational bands of B820 are present together with some absorption of B777 and, presumably, a weak absorption of the upper dimer component of B820 at ∼790 nm.[19] For OG concentrations larger than 1.2 and up to 5% (spectra 7 to 9), the absorption of B777 becomes stronger, while that of B820 decreases. At 5% OG (spectrum 9), only the band of B777 remains with a maximum at 778 nm and a width of ∼770 cm^{-1}, a behavior very similar to that of BChl-*a* in glasses[20] and detergents[19] (maximum at ∼780 nm and widths of ∼500−800 cm^{-1}, depending on the host). These widths are much larger than those of B820 and B873, probably because the latter two complexes are more ordered than B777 and yield narrower inhomogeneous bands.

To test the presence of the various species in more detail, we have measured fluorescence spectra, plotted in Figure 2, for various percentages of OG detergent. They have been recorded by exciting B820 and B777 in their absorption maxima at 825 and 780 nm, respectively. Spectrum 1, which is that of "pure" B873 excited at 825 nm, shows only a single emission band at 905 nm. The same fluorescence spectrum is obtained when exciting at 780 nm (not shown). In the absence of OG detergent, there is no emission from B777 or B820. For a concentration of 0.6% OG, for which the absorption spectrum in Figure 1 was identical to that of "pure" B873, the fluorescence spectrum shows two emission bands for excitation at 825 nm: a stronger one at 905 nm arising from B873 and a weaker one at ∼830 nm arising from B820. By exciting B777 at 780 nm, even a third emission band is observed at ∼785 nm (spectra 2 and 3). Apparently, these fluorescence spectra are very sensitive to the state of aggregation; they show that at very low OG detergent concentrations the three forms B873, B820, and B777 already coexist. For a concentration of 1.2% OG, the absorption spectrum had one band corresponding to the B820 dimer, whereas the fluorescence spectra demonstrate the simultaneous presence of both B820 and B777 (spectra 4 and 5). Similarly, the absorption spectrum for 5% OG shows only B777, whereas we again see two peaks in the fluorescence spectra, one belonging to B777 for excitation at 780 nm and one belonging to B820 for excitation at 825 nm (spectra 6 and 7). Neither from the absorption nor from the fluorescence spectra it is possible to determine whether "free" BChl is also present in the samples, because the spectra of B777 and "free" BChl are

9774 *J. Phys. Chem. B, Vol. 103, No. 44, 1999*

Creemers et al.

very similar. From results obtained for the optical homogeneous line width as a function of temperature and delay time, however, we concluded that all the detectable BChl-*a* in our samples is bound to the protein, i.e., it is B777.[11]

3.2 Fluorescence Line Narrowing: Identification of Low-Frequency Modes and Absence of "Downhill" Energy Transfer. Fluorescence line narrowing spectra of B820 and B777 at 1.6 K (up to 20 nm, i.e., $\sim$280−300 cm^{-1} to the red from the excitation wavelength) are depicted in Figure 3a,b for various excitation wavelengths λ_{exc}. The spectra of B820 (Figure 3a) are characterized by a low-frequency mode at $\sim$19 cm^{-1}, a broad emission peak at $\sim$60−80 cm^{-1}, and a long tail that extends beyond 1000 cm^{-1}. B777 (Figure 3b) shows a low-frequency mode similar to B820, but at a slightly higher frequency of $\sim$25 cm^{-1}. The broad peak appears at $\sim$60−90 cm^{-1} and the tail is less extended than in B820. We attribute the low-frequency modes to motions of the whole subunit within the micelle formed by the OG detergent. The difference in their frequencies can be caused by the difference in masses involved in the motions of B820 and B777. The latter, in addition, shows a sharp peak at $\sim$190 cm^{-1}, which is also observed for BChl-*a* in organic glasses[19,20] but not in the B820 dimer. Thus, we attribute it to monomeric BChl-*a*. This peak is not visible in the fluorescence spectra excited in the red wing of the absorption band (Figure 3b, top) because of the lower signal-to-noise ratio. Notice that the shape of the fluorescence spectra in Figure 3a,b changes when tuning the excitation wavelength across the absorption band. For λ_{exc} on the blue wing, the broad peak lies further away from the excitation wavelength than for λ_{exc} on the red wing because vibrational bands are excited at higher frequencies. Modes with frequencies larger than $\sim$200 cm^{-1} are probably hidden under the long and weak tail of the FLN spectra. Femtosecond spectroscopic experiments on B820 at room temperature show oscillations with frequencies not only between 20 and 200 cm^{-1},[21−23] but even up to 730 cm^{-1}.[23]

The positions of the low-frequency modes at 19 and 25 cm^{-1} in the emission spectra, λ_{em}, as a function of excitation wavelength λ_{exc} obey a linear dependence with dλ_{em}/dλ_{exc} = 1 (not shown). Thus, the energy difference between the emission and the excitation wavelength remains constant across the absorption band, which proves an earlier conclusion that "downhill" energy transfer (ET) does not occur among B820 subunits;[13] the same is true for B777. These findings differ from those for the B800 band of the LH2 complex of *Rhodobacter sphaeroides*[24,25] and the subcore complexes of PSII RC of green plants,[26] where dλ_{em}/dλ_{exc} = 1 holds only in the red wing. Toward the blue side of the band, λ_{em} becomes constant as a function of λ_{exc} because of fast "downhill" energy transfer within the band.

3.3 Hole Burning: Determination of Phonon Sidebands and Photoproducts. Hole burning experiments performed on the two subunits of LH1 have demonstrated that the B820 and B777 bands are inhomogeneously broadened at low temperature.[27] Figure 4a,b illustrates the spectral changes occurring as a consequence of burning deep, power-broadened holes in these bands. A zero-phonon hole in B820, resonant with the burn wavelength at λ_b = 823 nm, is shown as a sharp line in Figure 4a and enlarged in the inset. Its depth is D = 12% and its width $\Gamma_{hole} \sim$ 0.8 cm^{-1}. The phonon side hole, appearing simultaneously with the zero-phonon hole, has a width of $\sim$50 cm^{-1} and lies $\sim$20 cm^{-1} to the red side of the burned hole. This frequency is very similar to that of the 19 cm^{-1} low-frequency mode found by fluorescence line narrowing (section 3.2).[19] We attribute the asymmetry in the shape of the phonon side holes

in Figure 4a,b to burning into higher frequency vibrations. Low-frequency modes of $\sim$20 cm^{-1} were also observed for the B850 band of LH2 and the B870 band of LH1 by Small and co-workers.[28]

On the blue side of the zero-phonon hole, there is a broad antihole caused by absorption of a "photoproduct" created during burning. Its maximum lies at $\sim$816 nm, i.e., $\sim$100 cm^{-1} from λ_b. The energy difference between the side hole and the antihole is thus $\sim$120 cm^{-1}. Since the photoproduct (or antihole) is located within the B820-absorption band and its position shifts with burning wavelength (results not shown), we attribute it to a slightly different conformation of the B820 dimer and not to a chemically new species (see below). From triplet-minus-singlet spectra at 77 K reported in the literature[29] it was concluded that upon excitation of B820 at 825 nm, not only the triplet state of B820 is formed but also a "new monomer" absorbing at 809 nm, i.e., at $\sim$240 cm^{-1} to the blue of the excitation wavelength. Since this frequency is much larger than the 100 cm^{-1} found here, we conclude that the "photoproduct" created by hole burning is not the "new monomer" of ref 29. We have not detected the higher lying exciton (dimer) transition of B820, expected to appear as a weak satellite hole at $\sim$500 cm^{-1}, because the hole burning spectra were only scanned up to $\sim$400 cm^{-1} to the blue side of the burned hole.

The hole burning results obtained for B777 are similar to those for B820 (Figure 4b). The power-broadened zero-phonon hole (see inset) has a width $\Gamma_{hole} \sim$ 0.8 cm^{-1} and a depth D = 20%. The phonon side hole is $\sim$25 cm^{-1} to the red of the zero-phonon hole, in agreement with the value of the low-frequency mode in Figure 3b. The antihole or "photoproduct" absorbs $\sim$120 cm^{-1} to the blue of the zero-phonon hole. Thus, the energy difference between the side hole and the antihole is $\sim$145 cm^{-1}, which is only slightly larger than that found for B820. Moreover, the antihole of B777 is broader than that of B820, in agreement with the larger inhomogeneous band of B777 (see also Figure 1).

We note that the energy differences between the spectral positions of the holes burned in B820 and B777 and their respective "photoproducts" are very similar to the $\sim$100 cm^{-1} previously obtained by hole burning for magnesium porphin in an *n*-octane crystal[30] and for BChl-*a* in glasses.[20] We believe that not only in Mg−porphin and BChl-*a* in glasses, but also in the B820 and B777 subunits, it is the external ligation of the Mg atom which, after hole burning, has changed.

3.4 Dependence of the "Effective" Homogeneous Line Width Γ'_{hom} on Excitation Wavelength and Temperature. The "effective" homogeneous line width Γ'_{hom} was obtained by measuring the hole width Γ_{hole} as a function of burning fluence density Pt_b/A and extrapolating the values of Γ_{hole} to $Pt_b/A \rightarrow$ 0 (see also section 2.3). This is illustrated in Figure 5 for B820 at 1.2 K where, under the experimental conditions given, $\Gamma'_{hom} \sim$ 0.6 GHz. In a similar experiment on B777, $\Gamma'_{hom} \sim$ 0.5 GHz. Interestingly, the burning fluence densities that had to be used for B777 were about a factor of 10 lower than for B820, implying that the HB mechanism in the monomer is more efficient than in the dimer. A possible explanation could be that the BChl-*a* dimer in B820 is more rigidly constrained in its conformation than the BChl-*a* monomer in B777 because the surrounding protein in B820 consists of two α-helices, instead of one as in B777. It is, therefore, more difficult to burn B820 and switch it into another conformation.

The value of Γ'_{hom} as a function of excitation wavelength λ_{exc} has been plotted in Figure 6 for B820 at 1.2 and 4.2 K, and a delay time between burning and probing of t_d = 130 s. A

Spectral Hole Burning and Fluorescence Line Narrowing

J. Phys. Chem. B, Vol. 103, No. 44, 1999 **9775**

similar behavior was observed for B777 (not shown). At a given temperature, Γ'_{hom} is constant over the whole absorption band which proves that, in agreement with our FLN experiments (section 3.2), there is no detectable "downhill" energy transfer (ET) among the subunits. On the other hand, when the temperature is increased from 1.2 to 4.2 K, Γ'_{hom} increases by a factor of about 5, which is an indication that the value of Γ'_{hom} is dominated by "pure" dephasing and/or spectral diffusion. This can be understood from the following equation:[15−19,24,31]

$$\Gamma'_{hom} = \frac{1}{2\pi T_1} + \frac{1}{\pi T_2^* \, (T, t_d)} \tag{3}$$

where T_1 is the lifetime of the first electronically excited state and $T_2^* \, (T, t_d)$ takes into account "pure" dephasing and spectral diffusion. The first term in eq 3 consists, in general, of two terms, $(T_1)^{-1} = (\tau_{fl})^{-1} + (\tau_{ET})^{-1}$, with τ_{fl} the intrinsic fluorescence lifetime of the probe molecule in the absence of ET and $(\tau_{ET})^{-1}$ the energy transfer rate.[25,32] In our case, $T_1 = \tau_{fl}$. The second term in eq 3 is related to pigment−protein interactions which cause fluctuations of the optical transition due to phonon scattering; thus, T_2^* depends on temperature. The results of Figure 6 are consistent with such a picture. Furthermore, in glasses[16−18] and proteins[11,33] T_2^* may also depend on t_d, the delay time between burning and probing the hole. Since the value of Γ'_{hom}, at a given temperature and delay time, is slightly higher for B820 than for B777, it suggests that the BChl-*a* dimer in B820 is more strongly coupled to its surrounding protein than the BChl-*a* monomer in B777. In contrast to the small values of $\Gamma'_{hom} = 0.5−2.5$ GHz found here for the LH1 subunits (Figure 6), the values found for the B800 band of LH2 are 2 orders of magnitude larger (60 to 250 GHz).[24,25] Furthermore, the latter do not depend on temperature (at least for $T \leq 30$ K) but do vary with excitation wavelength and are, therefore, dominated by fast "downhill" energy transfer. Their transfer times decrease from the red (2.5 ps) to the blue wing (850 fs) of the B800 band at low temperatures.[24,25]

If the optical dephasing in the far red wing of the bands of the B850 and B870 complexes would be determined by that of the B820 dimer subunits, one would predict from our results a dephasing time of ∼130 ps at 4.2 K corresponding to $\Gamma'_{hom} \approx 2.5$ GHz in Figure 6. In refs 28 and 34, however, much shorter dephasing times of 5−7 ps were reported, which were attributed to scattering from the lowest exciton band. When making a comparison, it may be relevant that the burning fluence densities used in the present study are a factor 10^5 lower than those of ref 28.

4. Conclusions

We have shown by means of high-resolution spectroscopy at liquid He temperatures that the LH1 complex of *Rs. rubrum G9* (B873 aggregate) dissociates in two steps, first to B820 (with ∼1% OG) and then to B777 (with ∼5% OG) when adding OG detergent to it, and that the monomer and the dimer always coexist in OG solutions. The absorption band of B820 is much narrower than that of B777 (320 vs 770 cm^{-1}), probably because the B820 dimer is more ordered than the B777 monomer.

Hole burning (HB) experiments demonstrate that the spectral positions of the "photoproducts" of B820 and B777 are qualitatively similar to those previously found for BChl-*a* in glasses[20] and Mg−porphin in *n*-octane crystals.[30] We conclude that in both subunits a change in the external ligation of the central Mg atom in the BChl-*a* molecule occurs with respect to the surrounding protein. Since the quantum yield for this process

appears to be an order of magnitude larger for B777 than for B820, we believe that the B777 monomer has a weaker coupling to the protein than the B820 dimer.

We have further found that "downhill" energy transfer (ET) does not take place either within the B820 or within the B777 absorption bands. As a consequence, the distance between the subunits must be larger than the critical Förster radius for ET[32] (this is certainly correct if the micelles formed by the detergent do not contain more than one subunit and/or the subunits have the wrong orientations with respect to each other). Because of the absence of fast "downhill" ET, the value of the "effective" homogeneous line width Γ'_{hom} is rather small, of the order of 0.5 to a few GHz at 1.2−4.2 K. Since the rate corresponding to an intrinsic fluorescence decay time of 2−3 ns is about 0.05− 0.07 GHz, we conclude that the principal contribution to Γ'_{hom} arises from optical dephasing and/or spectral diffusion. The small size of these subunits makes them interesting model systems for studying structural relaxation in proteins over many orders of magnitude in time.[11]

References and Notes

(1) Van Grondelle, R.; Dekker, J. P.; Gillbro, T.; Sundström, V. *Biochim. Biophys. Acta* **1994**, *1187*, 1. Fleming, G. R.; van Grondelle, R. *Phys. Today* **1994**, *47*, 48.

(2) Karrasch, S.; Bullough, P. A.; Ghosh, R. *EMBO J.* **1995**, *14*, 631.

(3) McDermott, G.; Prince, S. M.; Freer, A. A.; Hawthornthwaite-Lawless, A. M.; Papiz, M. Z.; Cogdell, R. J.; Isaacs, N. W. *Nature* **1995**, *374*, 517.

(4) Miller, J. F.; Hinchigeri, S. B.; Parkes-Loach, P. S.; Callahan, P. M.; Sprinkle, J. R.; Loach, P. A. *Biochemistry* **1987**, *26*, 5055.

(5) Parkes-Loach, P. S.; Sprinkle, J. R.; Loach, P. A. *Biochemistry* **1988**, *27*, 2718.

(6) Visschers, R. W.; Chang, M. C.; van Mourik, F.; Parkes-Loach, P. S.; Heller, B. A.; Loach, P. A.; van Grondelle, R. *Biochemistry* **1991**, *30*, 5734.

(7) Ghosh, R.; Hauser, H.; Bachofen, R. *Biochemistry* **1988**, *27*, 1004.

(8) Chang, M. C.; Callahan, P. M.; Parkes-Loach, P. S.; Cotton, T. M.; Loach, P. A. *Biochemistry* **1990**, *29*, 421.

(9) Parkes-Loach, P. S.; Michalski, T. J.; Bass, W. J.; Smith, U.; Loach, P. A. *Biochemistry* **1990**, *29*, 2951.

(10) Sturgis, J. N.; Robert, B. *J. Mol. Biol.* **1994**, *238*, 445.

(11) Creemers, T. M. H.; Störkel, U.; Musa, S.; Visschers, R. W.; Völker, S., to be published.

(12) Van Mourik, F.; Visschers, R. W.; van Grondelle, R. *Chem. Phys. Lett.* **1992**, *193*, 1.

(13) Visschers, R. W.; van Mourik, F.; Monshouwer, R.; van Grondelle, R. *Biochim. Biophys. Acta* **1993**, *1141*, 238.

(14) Visschers, R. W.; Nunn, R.; Calkoen, F.; van Mourik, F.; Hunter, C. N.; Rice, D. W.; van Grondelle, R. *Biochim. Biophys. Acta* **1992**, *1100*, 259.

(15) Wannemacher, R.; Koedijk, J. M. A.; Völker, S. *Chem. Phys. Lett.* **1993**, *206*, 1.

(16) Koedijk, J. M. A.; Wannemacher, R.; Silbey, R. J.; Völker, S. *J. Phys. Chem.* **1996**, *100*, 19945.

(17) Creemers, T. M. H.; Koedijk, J. M. A.; Chan, I. Y.; Silbey, R. J.; Völker, S. *J. Chem. Phys.* **1997**, *107*, 4797.

(18) Den Hartog, F. T. H.; Van Papendrecht, C.; Silbey, R. J.; Völker, S. *J. Chem. Phys.* **1999**, *110*, 1010.

(19) Van der Toorn, J.-G. C.; Creemers, T. M. H.; Silbey, R. J.; Völker, S., to be published.

(20) Van der Laan, H.; Smorenburg, H. E.; Schmidt, Th.; Völker, S. *J. Opt. Soc. Am. B* **1992**, *9*, 931.

(21) Kumble, R.; Palese, S.; Visschers, R. W.; Dutton, P. L.; Hochstrasser, R. M. *Chem. Phys. Lett.* **1996**, *261*, 396.

(22) Yu, J.-Y.;Nagasawa, Y.; van Grondelle, R.; Fleming, G. R. *Chem. Phys. Lett.* **1997**, *280*, 404.

(23) Diffey, W. M.; Homoelle, J.; Edington, M. D.; Beck, W. F. *J. Phys. Chem. B* **1998**, *102*, 2776.

(24) Van der Laan, H.; De Caro, C. A.; Schmidt, Th; Visschers, R. W.; van Grondelle, R.; Fowler, G. J. S.; Hunter, C. N.; Völker, S. *Chem. Phys. Lett.* **1993**, *212*, 569.

(25) De Caro, C. A.; Visschers, R. W.; van Grondelle, R.; Völker, S. *J. Phys. Chem.* **1994**, *28*, 10584.

(26) Den Hartog, F. T. H.; Dekker, J. P.; van Grondelle, R.; Völker, S. *J. Phys. Chem. B* **1998**, *102*, 11007, and references therein.

(27) De Caro, C. A.; Visschers, R. W.; van Grondelle, R.; Völker, S. *J. Lumin*. **1994**, *58*, 149.

(28) Reddy, N. R. S.; Picorel, R.; Small, G. J. *J. Phys. Chem.* **1992**, *96*, 6458.

(29) Van Mourik, F.; van der Oord, C. J. R.; Visscher, K. J.; Parkes-Loach, P. S.; Loach, P. A.; Visschers, R. W.; van Grondelle, R. *Biochim. Biophys. Acta* **1991**, *1059*, 111.

(30) Dicker, A. I. M.; Johnson, L. W.; Völker, S.; van der Waals, J. H. *Chem. Phys. Lett.* **1983** *100*, 8.

(31) Völker, S. In *Relaxation Processes in Molecular Excited States*; Fünfschilling, J., Ed.; Kluwer: Dordrecht, 1989; pp 113−242. Völker, S. *Annu. Rev. Phys. Chem.* **1989**, *40*, 499, and references therein.

(32) Förster, Th. *Ann. Phys. (Leipzig)* **1948**, *2*, 55. Förster, Th. In *Modern Quantum Chemistry,* Part III; Sinanoglu, O., Ed.; Academic Press: New York, 1965; p 93.

(33) Den Hartog, F. T. H.; Van Papendrecht, C.; Störkel, U.; Völker, S. *J. Phys. Chem. B* **1999**, *103*, 1375.

(34) Reddy, N. R. S.; Cogdell, R. J.; Zhao, L.; Small, G. J. *Photochem. Photobiol.* **1993**, *57*, 35.